THE JOURNAL OF PHYSICAL CHEMISTRY Letters

Letter

pubs.acs.org/JPCL

Adjusting the Local Arrangement of π-Stacked Oligothiophenes through Hydrogen Bonds: A Viable Route to Promote Charge Transfer

Hongguang Liu, Éric Brémond, Antonio Prlj, Jérôme F. Gonthier, and Clémence Corminboeuf*

Institut des Sciences et Ingénierie Chimiques, Ecole Polytechnique Fédérale de Lausanne, CH-1015 Lausanne, Switzerland

Supporting Information

ABSTRACT: We show that substituting quaterthiophene cores with strong H-bond aggregators, such as urea groups, provides an efficient way to adjust the mutual in-plane displacements of the semiconducting units and promote charge transfer. Our 2-D structure−property mapping reveals that the insertion of substituents induces up to 2.0 Å longitudinal and transversal displacements between the π-conjugated moieties. Some of these relative displacements lead to improved cofacial orbital overlaps that are otherwise inaccessible due to Pauli repulsion. Our results also emphasize that the fine-tuning of in-plane displacements is more effective than achieving "tighter" packing to promote charge-transfer properties.

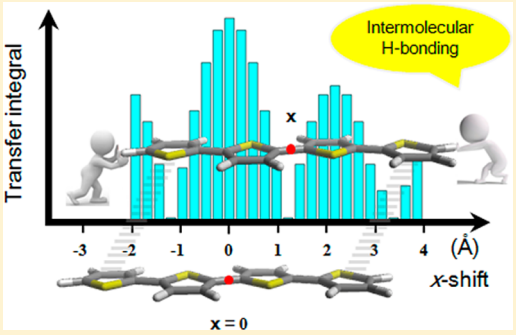

SECTION: Molecular Structure, Quantum Chemistry, and General Theory

Improving and controlling the performance of organic semiconducting materials constitutes a vibrant research field.[1,2] Among the most versatile p-type organic semiconductors, oligothiophenes display considerable potential as low-cost materials for solution-processed solar cells and field-effect transistors with good air stability.[3−8] Akin to oligoacenes, crystalline oligothiophenes (e.g., quaterthiophenes) and alkyl derivatives adopt a herringbone packing motif[9−14] (less π-orbital overlap) thanks to an increased number of C−H···π forces[15,16] and a reduction in Pauli repulsion[17−19] (i.e., exchange energy) relative to the face-to-face orientation. (See the Supporting Information.) However, charge-carrier mobility is largely dependent on the relative displacement of the π-conjugated cores: larger π-overlap generally results in better transport properties, the upper limit of which coincides with a perfect cofacial stack.[20−22] In this context, efforts have been placed on promoting good π-overlap to achieve enhanced charge carrier mobilities.[23,24] While discotic systems,[22,25] involving large flat polyaromatic cores, already display a sizable stacking surface, achieving good orbital overlap in flexible longitudinal oligomer chains is inherently more challenging. Quaterthiophene (QT) flanked with flexible hydrogen-bonded lateral functional groups can self-assemble into 1-D fibers in solution, with the oligothiophene moieties being π-stacked.[26−29] While the "H-bond aggregators" do not directly contribute to enhance the charge mobility in 1-D aggregates,[30−33] they do play a vital role in controlling the molecular arrangement and confining the QT segments. Despite such capabilities, a detailed relationship between the relative displacements induced by hydrogen-bonded lateral components and the charge mobility has yet to be established.[34−36] In fact, constructing organic molecules with π-stacked arrangement "at will" remains a difficult task.[37,38] Our objective here is to determine the capability of attractive hydrogen-bonding interactions to partially overcome the Pauli repulsion associated with cofacial π-electron clouds and stabilize otherwise unstable relative conformations. In particular, this work provides a quantitative one-to-one relationship between the achievable in-plane longitudinal and transversal displacements for different pairs of substituted quaterthiophene dimers (Figure 1) and the computed hole transfer integrals (t), on which the charge-transport properties strongly depend. (See the Supporting Information for details.) Here the focus is placed on parallel (displaced) QT dimers substituted with strong hydrogen-bond donor/acceptor groups such as alkylamides and alkylureas.

Intermolecular packing arrangements are best illustrated by 2-D plots displaying the relative translations in the long (x) and short (y) axes (Figure 2a). The surface plot in Figure 2c clearly identifies the energetically favored (red) and disfavored (blue) pair arrangements of bare quaterthiophenes (**1**) confined in a π-stacked conformation. As expected, the smallest binding energy (i.e., the most repulsive configuration) corresponds to the perfect cofacial stack (0,0), whereas the local minimum coincides with a large longitudinal displacement (x = 1.4 Å), with no translation along the y axis. In sharp contrast, the transfer integral is maximal (red) at (0,0) and cancels proximate to the local energy minimum (blue region). This raises a key question: can insertion of hydrogen-bonded substituents overcome the

Received: May 28, 2014
Accepted: June 17, 2014
Published: June 17, 2014

   dx.doi.org/10.1021/jz501078s | J. Phys. Chem. Lett. 2014, 5, 2320−2324

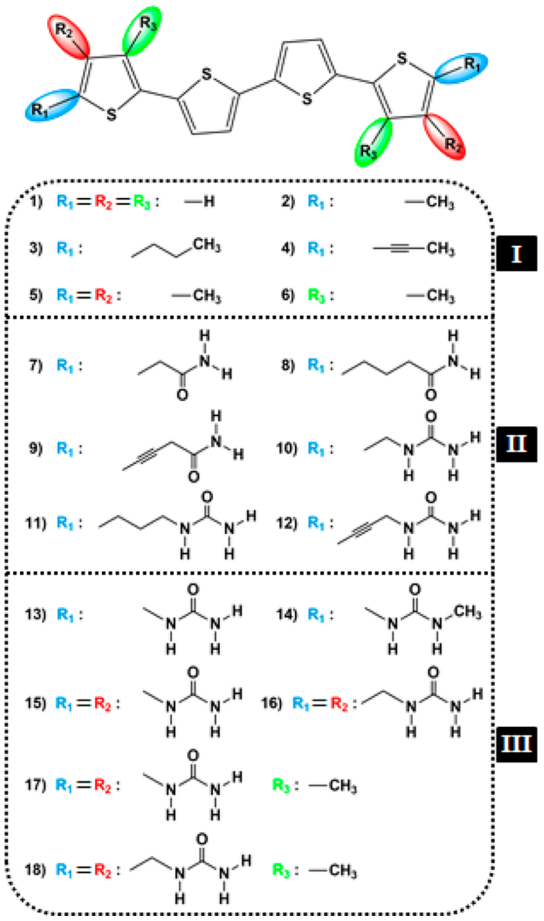

Figure 1. Illustrative QT derivatives with substitution patterns at R_1, R_2, or R_3. If not specified, R_1, R_2, or R_3 corresponds to −H.

dichotomy magnified by Figure 2b,c and assist in shifting the geometry toward more promising regions?

The exhaustive exploration of the chemical space spanned by all substituted oligothiophenes is obviously not feasible. Among myriad possibilities (see Figure 1 and Supporting Information for additional examples), three illustrative categories of substitution patterns are discussed here: (1) aliphatic and acetylenic side chains [$-CH_3$, $-CH_2-CH_2-CH_3$, and $-C\equiv C-CH_3$, i.e., pure dispersive interactions]; (2) alkylamide or alkylurea (i.e., H-bond substituents) groups attached to R_1 via an aliphatic or acetylenic linker; and (3) pure hydrogen-bond substituents or substitution at multiple positions.

The first class of substituted dimers, which lack hydrogen-bonds (i.e., **2**−**6**) and are generally known to adopt herringbone packing motifs,[10−14] shows no advantage over the reference system (**1**): the local energy minimum is located in the same region (with x = 1.4 Å and y = 0 Å) and results in no enhancement of the charge-transfer integral (~0.11 to 0.15 eV). Similarly, the intermolecular distance (i.e., z given in Figure 3a) is negligibly affected and remains around 3.34 Å. Inserting substituents belonging to the second category causes spectacular shifts along the x axis up to x = 3.4 Å (a shift of up to 2.0 Å!). Unfortunately, such a large translation overshoots the desired zone characterized by an increased orbital overlap and transfer integrals located at x = 2.25 Å. This second class of dimer aggregates also highlights that intermolecular distance adjustments are relevant only after controlling the subtle in-plane relative displacements: the intermolecular distance in **9**

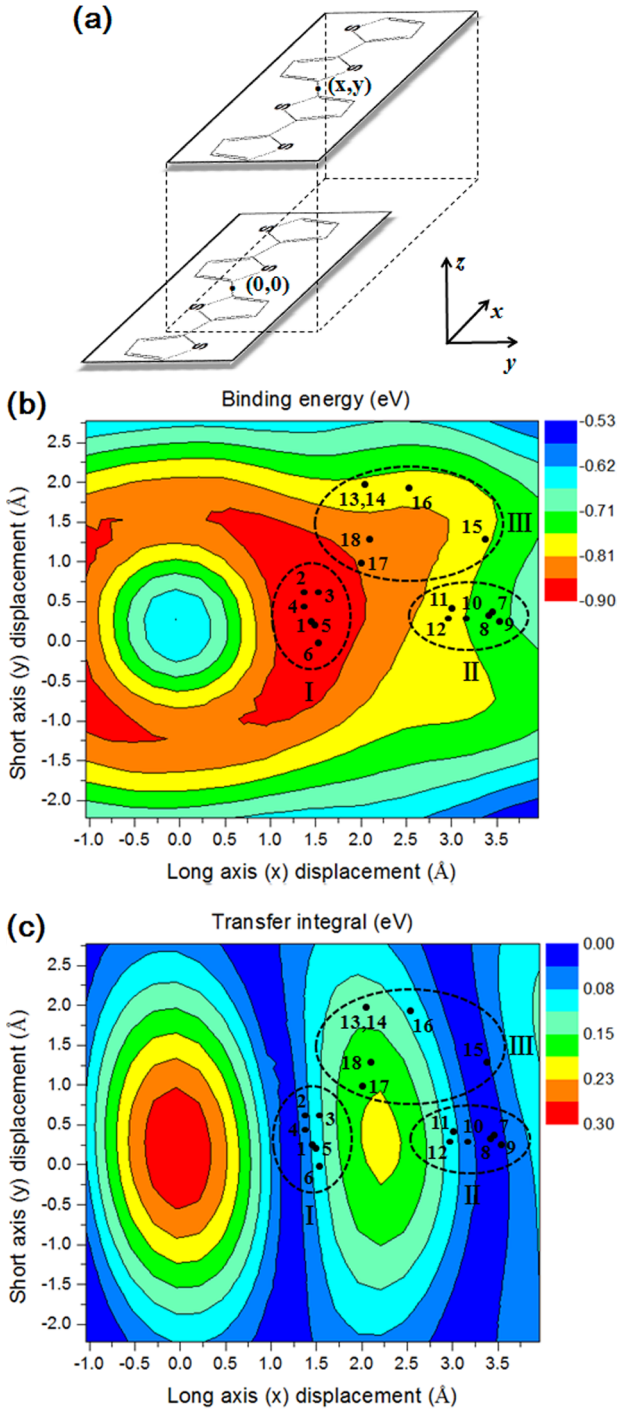

Figure 2. (a) Illustration of the QT cofacial stack showing the undergoing translations along x and y axes with a step length of 0.25 Å. The interplane distance z is fixed at 3.55 Å. (b) Landscapes of binding energies (PBE0-dDsC/def2-SVP) and (c) hole-transfer integrals (PBE0/DZP) for QT dimer as a function of stacking geometry (z = 3.55 Å). For clarity, we have reported here the absolute value of transfer integral because the sign is not relevant to the transfer properties in the hopping regime.[39] Black dots and labels indicate the PBE0-dDsC/def2-SVP optimized geometries of dimeric QT derivatives in Figure 1.

(3.18 Å) is significantly shorter than in **12** (3.26 Å), yet the former exhibits the worst possible overlap and transfer integral (t = 0 eV) owing to a too pronounced displacement along x (Figure 2). It is worth noting that the only investigated

dx.doi.org/10.1021/jz501078s | J. Phys. Chem. Lett. 2014, 5, 2320−2324

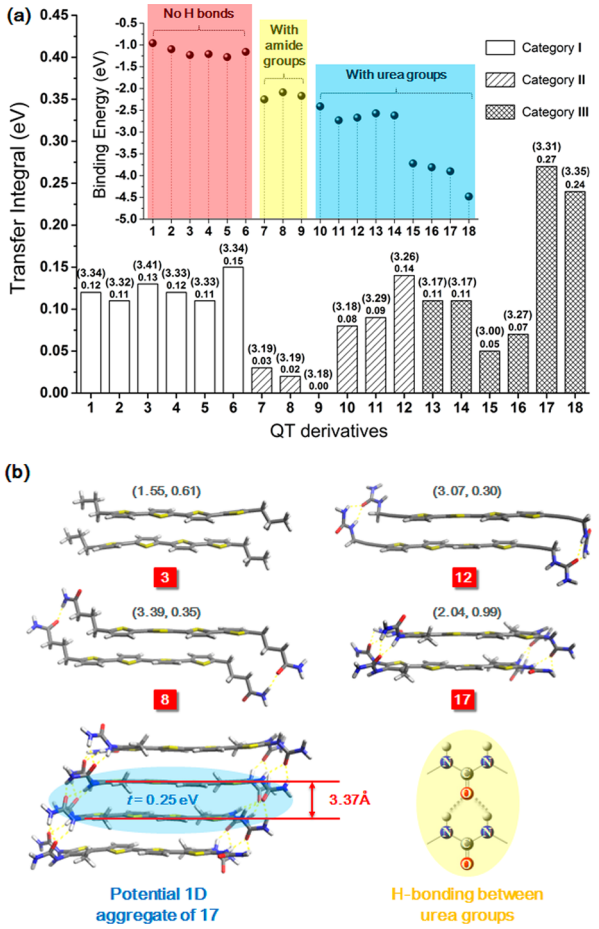

Figure 3. (a) Hole transfer integrals for dimeric QT derivatives optimized at the PBE0-dDsC/def2-SVP level. Binding energies at the same level are plotted as an inset. Value in the parentheses represents the interplane distance (in angstroms) between the thiophene moieties. (b) Representative dimer structures and **17** fully optimized in the tetramer geometry at the same level.

substituents capable of promoting backward longitudinal displacement toward x = 0 Å arise from the asymmetric combination of substituents, which is unfavorable experimentally (see Supporting Information, entry **26** in Scheme S1). The third category beautifully demonstrates the subtle benefits of inserting strong hydrogen-bond aggregators to promote large longitudinal and lateral displacements. The most spectacular overall displacements (as compared with **1**) are induced by the addition of one or two urea groups per QT unit such as in **13**, **14**, and **16**. Still, the potential advantage anticipated by a 0.5 Å shift along the longitudinal direction is canceled by the too pronounced lateral displacement that is not favorable to the targeted orbital overlap. In **13** and **14**, the more compressed packing (z = 3.17 Å) along with the rigid geometrical constraints imposed by the formation of the four hydrogen bonds is not constructive. Increasing the number of hydrogen bonds through the insertion of another urea group in the β positions (e.g., **15**) does not help or even deteriorate the overlap. In fact, the use of urea groups in both the α and β positions is valuable only with the synergistic presence of methyl groups in the R_3 position (e.g., **17**): the methyl groups help deplanarize the ureas in R_2 and immobilize the dimer in a much more favorable region (x = 2.0 Å, y = 1.0 Å, z = 3.31 Å). The subtle structural modifications induced by the methyl groups at R_3 are also evident when comparing **18** to **16**. The unique orientation provided by the substitution pattern of **17** yields charge-transfer integrals that have over twice the magnitude (0.27 eV) of ref 1. Yet again, the large intermolecular distances of both **17** and **18** demonstrate that achieving "tighter" packing is secondary to adjusting the in-plane relative displacements. This is somewhat unfortunate given that the latter displacements are much less intuitive to design a priori, compared to the packing distance.[27,40,41] The geometrical advantages characteristic of **17** still hold for larger stacks of QT and are not restricted to the static situation described by our density functional theory computations. (See Computational Details.) In fact, a Born–Oppenheimer molecular dynamics trajectory performed on the dimer and tetramer aggregates demonstrates that the averaged x, y, and t values are comparable to the static computation. (See Figure S3 in the Supporting Information.) Importantly as well, the key structural features present in **17** are compatible with the inclusion of solubilizing side chains that would be relevant experimentally.

In summary, we showed that "clipping" strong hydrogen-bond aggregators, such as urea groups, to quaterthiophene moieties enables the adjustment of the relative positions of the π-conjugated moieties, thus promoting enhanced charge-transport properties. Our 2-D structure–property mapping demonstrates that the insertion of hydrogen-bond substituents induces large lateral and longitudinal displacements that are otherwise inaccessible due to strong Pauli repulsion. Furthermore, this mapping illustrates that achieving "tighter" packing (e.g., shorter intermolecular distance) is only significant if fine-tuned relative longitudinal and lateral displacements are realized. As such, the actual challenge lies in the delivery of general guidelines to control the "in-plane" relative displacements between the quaterthiophene cores and to access the promising conformations. This realization relies on a subtle interplay between H bonds formed with suitable torsional angles and other attractive and repulsive noncovalent interactions (dispersion forces, electrostatics interactions, and Pauli repulsion). Thus, of great importance is that seemingly innocent substituents may actually have a significantly greater impact than originally anticipated. Given this knowledge, it appears that the synergistic exploitation of the steric hindrance brought by alkyl substitutions along with the formation of strong hydrogen bonds holds the key for rational design.

■ COMPUTATIONAL DETAILS

Dimer and tetramer geometries were optimized in a development version of Q-Chem[42] at the PBE0-dDsC/def2-SVP level, which has been shown to be reliable for noncovalently bound complexes.[43−47] The representative grid used to map the contour surface for transfer integrals and binding energies as a function of molecular x- and y-axis translations (Figure 2) was constructed from a dimer of bare quaterthiophene optimized at the same level. The relative monomer barycenters were then displaced (in x,y) on intervals of 0.25 Å at a fix interplane distance (z) of 3.55 Å. The PBE0-dDsC/def2-SVP binding energies were computed from the energy difference between the dimer and the monomers in the dimer geometries, with no correction for basis-set superposition error. Note that the use of other functionals (e.g., M06-2X;[48,49] see Supporting Information) leads to the same qualitative features as shown in Figure 2b,c. The charge transfer integrals for hole transport were computed at the PBE0/DZP level for each grid conformation as well as for the pairs of optimized substituted quaterthiophene derivatives.

dx.doi.org/10.1021/jz501078s | J. Phys. Chem. Lett. 2014, 5, 2320−2324

We used the direct quantum-mechanical approach implemented in ADF 2013[50−52] that is based on localized monomer orbitals in combination with a basis set orthogonalization procedure.[53]

■ ASSOCIATED CONTENT

Supporting Information

Details of the computation of the transfer integrals, SAPT0 analysis, 2-D structure−property mapping at the M06-2X level, additional substitution patterns and their effects on the transfer integral, and information on the Born−Oppenheimer molecular dynamics. This material is available free of charge via the Internet at http://pubs.acs.org.

■ AUTHOR INFORMATION

Notes

The authors declare no competing financial interest.

■ ACKNOWLEDGMENTS

Funding from the *European Research Council* (ERC Grants 306528, "COMPOREL"), the "secretariat d'état à l'éducation et à la recherche" (SER) within the framework of the COST action CM1002, and the Swiss National Science Foundation (no. 137666). We thank Holger Frauenrath and his group members for their inspiring experimental work.

■ REFERENCES

(1) Henson, Z. B.; Müllen, K.; Bazan, G. C. Design Strategies for Organic Semiconductors beyond the Molecular Formula. *Nat. Chem.* **2012**, *4*, 699−704.

(2) Sokolov, A. N.; Atahan-Evrenk, S.; Mondal, R.; Akkerman, H. B.; Sanchez-Carrera, R. S.; Granados-Focil, S.; Schrier, J.; Mannsfeld, S. C. B.; Zoombelt, A. P.; Bao, Z. N.; et al. From Computational Discovery to Experimental Characterization of a High Hole Mobility Organic Crystal. *Nat. Commun.* **2011**, *2*, 437/1−437/8.

(3) McCulloch, I.; Ashraf, R. S.; Biniek, L.; Bronstein, H.; Combe, C.; Donaghey, J. E.; James, D. I.; Nielsen, C. B.; Schroeder, B. C.; Zhang, W. M. Design of Semiconducting Indacenodithiophene Polymers for High Performance Transistors and Solar Cells. *Acc. Chem. Res.* **2012**, *45*, 714−722.

(4) McCulloch, I.; Heeney, M.; Bailey, C.; Genevicius, K.; MacDonald, I.; Shkunov, M.; Sparrowe, D.; Tierney, S.; Wagner, R.; Zhang, W. M.; et al. Liquid-Crystalline Semiconducting Polymers with High Charge-Carrier Mobility. *Nat. Mater.* **2006**, *5*, 328−333.

(5) Umeda, T.; Kumaki, D.; Tokito, S. Surface-Energy-Dependent Field-Effect Mobilities up to 1 cm^2/Vs for Polymer Thin-Film Transistor. *J. Appl. Phys.* **2009**, *105*, 024516/1−024516/5.

(6) Lee, M. J.; Gupta, D.; Zhao, N.; Heeney, M.; McCulloch, I.; Sirringhaus, H. Anisotropy of Charge Transport in a Uniaxially Aligned and Chain-Extended, High-Mobility, Conjugated Polymer Semiconductor. *Adv. Funct. Mater.* **2011**, *21*, 932−940.

(7) Elschner, C.; Schrader, M.; Fitzner, R.; Levin, A. A.; Bäuerle, P.; Andrienko, D.; Leo, K.; Riede, M. Molecular Ordering and Charge Transport in a Dicyanovinyl-Substituted Quaterthiophene Thin Film. *RSC Adv.* **2013**, *3*, 12117−12123.

(8) Poelking, C.; Cho, E.; Malafeev, A.; Ivanov, V.; Kremer, K.; Risko, C.; Brédas, J. L.; Andrienko, D. Characterization of Charge-Carrier Transport in Semicrystalline Polymers: Electronic Couplings, Site Energies, and Charge-Carrier Dynamics in Poly(bithiophene-alt-thienothiophene) [PBTTT]. *J. Phys. Chem. C* **2013**, *117*, 1633−1640.

(9) Siegrist, T.; Kloc, C.; Laudise, R. A.; Katz, H. E.; Haddon, R. C. Crystal Growth, Structure, and Electronic Band Structure of α-4T Polymorphs. *Adv. Mater.* **1998**, *10*, 379−382.

(10) Hotta, S.; Waragai, K. Alkyl-Substituted Oligothiophenes: Crystallographic and Spectroscopic Studies of Neutral and Doped Forms. *J. Mater. Chem.* **1991**, *1*, 835−842.

(11) Marseglia, E. A.; Grepioni, F.; Tedesco, E.; Braga, D. Solid State Conformation and Crystal Packing of Methyl-Substituted Quaterthiophenes. *Mol. Cryst. Liq. Cryst.* **2000**, *348*, 137−151.

(12) DiCésare, N.; Belletête, M.; Garcia, E. R.; Leclerc, M.; Durocher, G. Intermolecular Interactions in Conjugated Oligothiophenes. 3. Optical and Photophysical Properties of Quaterthiophene and Substituted Quaterthiophenes in Various Environments. *J. Phys. Chem. A* **1999**, *103*, 3864−3875.

(13) Macchi, G.; Milián Medina, B.; Zambianchi, M.; Tubino, R.; Cornil, J.; Barbarella, G.; Gierschner, J.; Meinardi, F. Spectroscopic Signatures for Planar Equilibrium Geometries in Methyl-Substituted Oligothiophenes. *Phys. Chem. Chem. Phys.* **2009**, *11*, 984−990.

(14) Macchi, G.; Botta, C.; Calzaferri, G.; Catti, M.; Cornil, J.; Gierschner, J.; Meinardi, F.; Tubino, R. Weak Forces at Work in Dye-Loaded Zeolite Materials: Spectroscopic Investigation on Cation-Sulfur Interactions. *Phys. Chem. Chem. Phys.* **2010**, *12*, 2599−2605.

(15) Williams, D. E.; Xiao, Y. Benzene, Naphthalene and Anthracene Dimers and Their Relation to the Observed Crystal Structures. *Acta Crystallogr., Sect. A* **1993**, *49*, 1−10.

(16) Tsuzuki, S.; Honda, K.; Azumi, R. Model Chemistry Calculations of Thiophene Dimer Interactions: Origin of π-Stacking. *J. Am. Chem. Soc.* **2002**, *124*, 12200−12209.

(17) Podeszwa, R.; Bukowski, R.; Szalewicz, K. Potential Energy Surface for the Benzene Dimer and Perturbational Analysis of π-π Interactions. *J. Phys. Chem. A* **2006**, *110*, 10345−10354.

(18) Grimme, S. Do Special Noncovalent π-π Stacking Interactions Really Exist? *Angew. Chem., Int. Ed.* **2008**, *47*, 3430−3434.

(19) Hohenstein, E. G.; Sherrill, C. D. Density Fitting and Cholesky Decomposition Approximations in Symmetry-Adapted Perturbation Theory: Implementation and Application to Probe the Nature of π-π Interactions in Linear Acenes. *J. Chem. Phys.* **2010**, *132*, 184111/1−184111/10.

(20) Brédas, J. L.; Calbert, J. P.; da Silva Filho, D. A.; Cornil, J. Organic Semiconductors: A Theoretical Characterization of the Basic Parameters Governing Charge Transport. *Proc. Natl. Acad. Sci. U. S. A.* **2002**, *99*, 5804−5809.

(21) Coropceanu, V.; Cornil, J.; da Silva, D. A.; Olivier, Y.; Silbey, R.; Brédas, J. L. Charge Transport in Organic Semiconductors. *Chem. Rev.* **2007**, *107*, 926−952.

(22) Feng, X. L.; Marcon, V.; Pisula, W.; Hansen, M. R.; Kirkpatrick, J.; Grozema, F.; Andrienko, D.; Kremer, K.; Müllen, K. Towards High Charge-Carrier Mobilities by Rational Design of the Shape and Periphery of Discotics. *Nat. Mater.* **2009**, *8*, 421−426.

(23) Moon, H.; Zeis, R.; Borkent, E. J.; Besnard, C.; Lovinger, A. J.; Siegrist, T.; Kloc, C.; Bao, Z. N. Synthesis, Crystal Structure, and Transistor Performance of Tetracene Derivatives. *J. Am. Chem. Soc.* **2004**, *126*, 15322−15323.

(24) Anthony, J. E. Functionalized Acenes and Heteroacenes for Organic Electronics. *Chem. Rev.* **2006**, *106*, 5028−5048.

(25) Wheeler, S. E. Controlling the Local Arrangements of π-Stacked Polycyclic Aromatic Hydrocarbons through Substituent Effects. *CrystEngComm* **2012**, *14*, 6140−6145.

(26) Marty, R.; Szilluweit, R.; Sanchez-Ferrer, A.; Bolisetty, S.; Adamcik, J.; Mezzenga, R.; Spitzner, E. C.; Feifer, M.; Steinmann, S. N.; Corminboeuf, C.; et al. Hierarchically Structured Microfibers of "Single Stack" Perylene Bisimide and Quaterthiophene Nanowires. *ACS Nano* **2013**, *7*, 8498−8508.

(27) Tevis, I. D.; Palmer, L. C.; Herman, D. J.; Murray, I. P.; Stone, D. A.; Stupp, S. I. Self-Assembly and Orientation of Hydrogen-Bonded Oligothiophene Polymorphs at Liquid-Membrane-Liquid Interfaces. *J. Am. Chem. Soc.* **2011**, *133*, 16486−16494.

(28) Stone, D. A.; Tayi, A. S.; Goldberger, J. E.; Palmer, L. C.; Stupp, S. I. Self-Assembly and Conductivity of Hydrogen-Bonded Oligothiophene Nanofiber Networks. *Chem. Commun.* **2011**, *47*, 5702−5704.

(29) Wall, B. D.; Diegelmann, S. R.; Zhang, S. M.; Dawidczyk, T. J.; Wilson, W. L.; Katz, H. E.; Mao, H. Q.; Tovar, J. D. Aligned Macroscopic Domains of Optoelectronic Nanostructures Prepared via Shear-Flow Assembly of Peptide Hydrogels. *Adv. Mater.* **2011**, *23*, 5009−5014.

(30) Balakrishnan, K.; Datar, A.; Naddo, T.; Huang, J. L.; Oitker, R.; Yen, M.; Zhao, J. C.; Zang, L. Effect of Side-Chain Substituents on Self-Assembly of Perylene Diimide Molecules: Morphology Control. *J. Am. Chem. Soc.* **2006**, *128*, 7390−7398.
(31) De Luca, G.; Liscio, A.; Nolde, F.; Scolaro, L. M.; Palermo, V.; Müllen, K.; Samorì, P. Self-Assembly of Discotic Molecules into Mesoscopic Crystals by Solvent-Vapour Annealing. *Soft Matter* **2008**, *4*, 2064−2070.
(32) Savage, R. C.; Orgiu, E.; Mativetsky, J. M.; Pisula, W.; Schnitzler, T.; Eversloh, C. L.; Li, C.; Müllen, K.; Samorì, P. Charge Transport in Fibre-Based Perylene-Diimide Transistors: Effect of the Alkyl Substitution and Processing Technique. *Nanoscale* **2012**, *4*, 2387−2393.
(33) Gesquière, A.; Abdel-Mottaleb, M. M. S.; De Feyter, S.; De Schryver, F. C.; Schoonbeek, F.; van Esch, J.; Kellogg, R. M.; Feringa, B. L.; Calderone, A.; Lazzaroni, R.; et al. Molecular Organization of Bis-Urea Substituted Thiophene Derivatives at the Liquid/Solid Interface Studied by Scanning Tunneling Microscopy. *Langmuir* **2000**, *16*, 10385−10391.
(34) Gsänger, M.; Oh, J. H.; Könemann, M.; Höffken, H. W.; Krause, A. M.; Bao, Z. N.; Würthner, F. A Crystal-Engineered Hydrogen-Bonded Octachloroperylene Diimide with a Twisted Core: An n-Channel Organic Semiconductor. *Angew. Chem., Int. Ed.* **2010**, *49*, 740−743.
(35) Zhang, M. X.; Zhao, G. J. Modification of n-Type Organic Semiconductor Performance of Perylene Diimides by Substitution in Different Positions: Two-Dimensional π-Stacking and Hydrogen Bonding. *ChemSusChem* **2012**, *5*, 879−887.
(36) Kolhe, N. B.; Devi, R. N.; Senanayak, S. P.; Jancy, B.; Narayan, K. S.; Asha, S. K. Structure Engineering of Naphthalene Diimides for Improved Charge Carrier Mobility: Self-Assembly by Hydrogen Bonding, Good or Bad? *J. Mater. Chem.* **2012**, *22*, 15235−15246.
(37) Sokolov, A. N.; Friščić, T.; Blais, S.; Ripmeester, J. A.; MacGillivray, L. R. Persistent One-Dimensional Face-to-Face π-Stacks within Organic Cocrystals. *Cryst. Growth Des.* **2006**, *6*, 2427−2428.
(38) Sokolov, A. N.; Friščić, T.; MacGillivray, L. R. Enforced Face-to-Face Stacking of Organic Semiconductor Building Blocks within Hydrogen-Bonded Molecular Cocrystals. *J. Am. Chem. Soc.* **2006**, *128*, 2806−2807.
(39) Vura-Weis, J.; Ratner, M. A.; Wasielewski, M. R. Geometry and Electronic Coupling in Perylenediimide Stacks: Mapping Structure-Charge Transport Relationships. *J. Am. Chem. Soc.* **2010**, *132*, 1738−1739.
(40) Curtis, M. D.; Cao, J.; Kampf, J. W. Solid-State Packing of Conjugated Oligomers: From π-Stacks to the Herringbone Structure. *J. Am. Chem. Soc.* **2004**, *126*, 4318−4328.
(41) Lan, Y. K.; Huang, C. I. Charge Mobility and Transport Behavior in the Ordered and Disordered States of the Regioregular Poly(3-hexylthiophene). *J. Phys. Chem. B* **2009**, *113*, 14555−14564.
(42) Shao, Y.; Molnar, L. F.; Jung, Y.; Kussmann, J.; Ochsenfeld, C.; Brown, S. T.; Gilbert, A. T. B.; Slipchenko, L. V.; Levchenko, S. V.; O'Neill, D. P.; et al. Advances in Methods and Algorithms in a Modern Quantum Chemistry Program Package. *Phys. Chem. Chem. Phys.* **2006**, *8*, 3172−3191.
(43) Perdew, J. P.; Burke, K.; Ernzerhof, M. Generalized Gradient Approximation Made Simple. *Phys. Rev. Lett.* **1996**, *77*, 3865−3868.
(44) Adamo, C.; Barone, V. Toward Reliable Density Functional Methods without Adjustable Parameters: The PBE0 Model. *J. Chem. Phys.* **1999**, *110*, 6158−6170.
(45) Steinmann, S. N.; Corminboeuf, C. Comprehensive Benchmarking of a Density-Dependent Dispersion Correction. *J. Chem. Theory Comput.* **2011**, *7*, 3567−3577.
(46) Steinmann, S. N.; Piemontesi, C.; Delacht, A.; Corminboeuf, C. Why are the Interaction Energies of Charge-Transfer Complexes Challenging for DFT? *J. Chem. Theory Comput.* **2012**, *8*, 1629−1640.
(47) Steinmann, S. N.; Corminboeuf, C. Exploring the Limits of Density Functional Approximations for Interaction Energies of Molecular Precursors to Organic Electronics. *J. Chem. Theory Comput.* **2012**, *8*, 4305−4316.
(48) Zhao, Y.; Truhlar, D. G. The M06 Suite of Density Functionals for Main Group Thermochemistry, Thermochemical Kinetics, Noncovalent Interactions, Excited States, and Transition Elements: Two New Functionals and Systematic Testing of Four M06-Class Functionals and 12 Other Functionals. *Theor. Chem. Acc.* **2008**, *120*, 215−241.
(49) Zhao, Y.; Truhlar, D. G. Density Functionals with Broad Applicability in Chemistry. *Acc. Chem. Res.* **2008**, *41*, 157−167.
(50) te Velde, G.; Bickelhaupt, F. M.; Baerends, E. J.; Guerra, C. F.; Van Gisbergen, S. J. A.; Snijders, J. G.; Ziegler, T. Chemistry with ADF. *J. Comput. Chem.* **2001**, *22*, 931−967.
(51) Guerra, C. F.; Snijders, J. G.; te Velde, G.; Baerends, E. J. Towards an Order-N DFT Method. *Theor. Chem. Acc.* **1998**, *99*, 391−403.
(52) SCM, Theoretical Chemistry. *ADF2013*; Vrije Universiteit: Amsterdam, The Netherlands, 2013.
(53) Valeev, E. F.; Coropceanu, V.; da Silva Filho, D. A.; Salman, S.; Brédas, J. L. Effect of Electronic Polarization on Charge-Transport Parameters in Molecular Organic Semiconductors. *J. Am. Chem. Soc.* **2006**, *128*, 9882−9886.